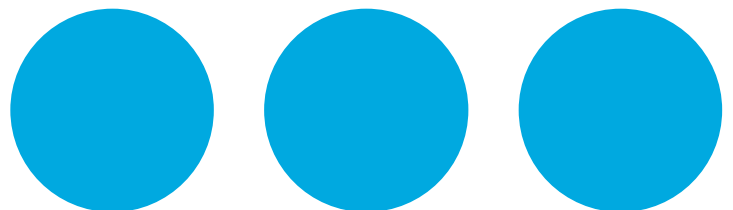


# Image-based Dosimetry for Yttrium-90 Microsphere Brachytherapy

Tim Fox, PhD, George Andl, MS, Peter Potrebko, PhD,  
Varian Medical Systems



## Table of Contents

Introduction	3
Quantitative <sup>90</sup> Y Imaging	3
<sup>90</sup> Y Dose Calculation Model	4
Phantom Study	4
References	7

## Introduction

Radioembolization of liver malignancies with  $^{90}\text{Y}$  microspheres is a form of brachytherapy that delivers radiation from  $\beta$ -emitting microspheres that are injected through the hepatic artery. The microspheres may be made of resin (SIR-Spheres<sup>®</sup>; Sirtex Medical Limited, Sydney, Australia) or glass (TheraSphere<sup>®</sup>; BTG, Ottawa, Canada). Yttrium-90 is a  $\beta$ -emitter with a mean range in tissue of 3.8 mm [1]. Ninety percent of the emitted energy is absorbed within a radius of 5.3 mm [2]. The microsphere delivered dose is analogous to a permanent brachytherapy implant.

Current practice uses manufacturer recommended prescription activity and dose calculations, derived from the Medical Internal Radiation Dose (MIRD) Committee of the Society of Nuclear Medicine, which are based on the size of the intended treatment volume [1,2]. The MIRD formalism assumes a uniform distribution of the activity throughout the injected areas of the liver and does not provide information about the actual distribution of microspheres in tumors and normal tissue.

Quantitative patient-specific  $^{90}\text{Y}$  dosimetry has been studied using bremsstrahlung single photon emission computed tomography (SPECT)/computed tomography (CT) and positron emission tomography (PET/CT) [3-5]. Voxel-based dosimetry models, such as the Local Deposition Method (LDM), have been developed that convert the activity distribution in  $^{90}\text{Y}$  SPECT and PET images to absorbed dose distributions [6]. The LDM method has been implemented within the yoSphere<sup>™</sup> image-guided Y90 dosimetry software and will be discussed in greater detail, along with SPECT/CT and PET/CT  $^{90}\text{Y}$  imaging, in the following sections.

## Quantitative $^{90}\text{Y}$ Imaging

The  $\beta$ -radiation emitted by  $^{90}\text{Y}$  interacts with body tissues and results in bremsstrahlung photons. Traditionally, SPECT/CT has been regarded as the gold-standard modality to image the biodistribution of this radionuclide. However, the low photon yield and continuous nature of the bremsstrahlung X-ray spectrum make SPECT imaging involving  $^{90}\text{Y}$  technically challenging [4]. For this paper,  $^{90}\text{Y}$  SPECT/CT images were acquired and reconstructed following the approach by Siman *et al.* [4]. The acquisition of  $^{90}\text{Y}$  SPECT was optimized using a primary energy window of 90-130 keV and a background compensation energy window of 310-400 keV on a Siemens Symbia SPECT/CT (Siemens Medical Solutions Inc. Malvern, PA). The SPECT images were acquired with a matrix size of 128 x 128, 4.8 mm pixel size, 28 s/view for 128 views over 360 degrees. SPECT images were reconstructed using the manufacturer's three-dimensional ordered-subset expectation maximization algorithm using 8 iterations with 16 subsets, geometric collimator response modeling, CT-based attenuation correction using effective energy of the imaging window, dual energy window-based scatter correction, and a 9.6 mm FWHM post-reconstruction Gaussian filter [4].

On the other hand,  $^{90}\text{Y}$  decay may result in emission of a positron-electron pair. Despite the branching ratio of pair-production being quite small, (~32 ppm), more recent studies have shown  $^{90}\text{Y}$  PET/CT to be feasible in phantoms and patients [5-7]. Advanced correction techniques for scatter, random, and attenuation effects that are clinically available for  $^{18}\text{F}$  PET can be directly applied to  $^{90}\text{Y}$  PET [8]. The  $^{90}\text{Y}$  PET images in this paper were acquired on a Siemens Biograph mCT Flow with a 30 min acquisition time using continuous motion of the patient table. PET images were reconstructed using the manufacturer's three-dimensional ordered-subset expectation maximization algorithm using a 4.1 mm pixel size, 1 iteration with 21 subsets, 5 mm Gaussian filter with point spread function resolution recovery, time-of-flight, and CT-based attenuation correction [7].

## $^{90}\text{Y}$ Dose Calculation Model

The RapidSphere™  $^{90}\text{Y}$  dose calculation uses the local deposition method (LDM) [3,9,10], which was previously demonstrated to be the most accurate when using SPECT and PET imaging [6,11]. In this technique,  $^{90}\text{Y}$   $\beta$ -particles released by decay within a voxel deposit all energy locally within the same voxel. This is an accurate approximation considering that the mean range of  $\beta$ -particles in tissue is 3.8 mm which is within the typical SPECT/PET voxel size. The absorbed dose within a voxel is where  $A$  = injected activity,  $LSF$  = lung shunt fraction,  $T_{1/2}$  =  $^{90}\text{Y}$  physical half-life (64.08 hours),  $E_{avg}$  = average  $\beta$ -particle energy per disintegration (0.935 MeV),  $C_{voxel}$  = counts within voxel,  $\Delta V$  = voxel volume,  $\rho$  = tissue density, and  $C_{total}$  = total counts within the patient (excluding the lungs). The only patient-specific parameters that need to be manually entered into the software prior to the dose calculation are the injected activity (GBq or mCi) and the lung shunt fraction (expressed as %). The default tissue density is set to that of soft tissue (1.04 g/cm<sup>3</sup>).

$$D_{voxel} = \frac{A (1 - LSF) T_{1/2} E_{avg}}{\Delta V \rho \ln(2) C_{total}}$$

## Phantom Study

Dosimetry using  $^{90}\text{Y}$  SPECT/CT and PET/CT was compared using a phantom study. The phantom consisted of two regions, a 10 cc gelatin suspension of  $^{90}\text{Y}$  microspheres (simulating a GTV) surrounded by a 200 cc plastic/gelatin region (simulating a segment of the liver). The GTV region was created by mixing a 5%-by-weight solution of gelatin with hot water and  $^{90}\text{Y}$  microspheres. This solution was stirred during rapid cooling within an ice-water bath resulting in a uniform distribution of microspheres. This was necessary to prevent microsphere sedimentation due to gravity. The total  $^{90}\text{Y}$  microsphere activity was 0.66 GBq with a prescription dose of 160 Gy. SPECT/CT and PET/CT imaging of the phantom was performed as inputs for the LDM conversion to dose within RapidSphere™ (Figure 1).



Figure 1: The SPECT/CT of the liver segment phantom which consists of two regions, a 10 cc gelatin suspension of  $^{90}\text{Y}$  microspheres (GTV) surrounded by a 200 cc plastic/gelatin region (liver segment). The GTV and liver segment are displayed in red and orange, respectively.

Figure 2 illustrates the dose-volume histograms of the GTV and Liver Segment for both SPECT/CT and PET/CT  $^{90}\text{Y}$  dosimetry. The dosimetric goals were to cover at least 98% of the GTV with the prescription dose ( $V160\text{Gy} \geq 98\%$ ) while keeping the mean dose to the rest of the segment (Segment – GTV) below 70 Gy. In this example, only the  $^{90}\text{Y}$  PET dosimetry was able to satisfy the dosimetric goals. In contrast to SPECT dosimetry, the PET dosimetry method calculated much higher local doses within the GTV that are characteristic of brachytherapy. This result is consistent with Elschot *et al* which demonstrated that time- of-flight PET-based  $^{90}\text{Y}$  dose estimates were more accurate than SPECT-based dose estimates which produced large underestimations in high-dose regions [12].



Figure 2: Dose-volume histograms for both SPECT (solid) and PET (dashed) dosimetry. The dosimetric goals were to cover at least 98% of the GTV with the prescription dose (V160Gy ≥ 98%) while keeping the mean dose to the rest of the segment (Segment – GTV) below 70 Gy. In this example, only the <sup>90</sup>Y PET dosimetry was able to satisfy the dosimetric goals. Also, the PET dosimetry method calculated much higher local doses within the GTV that are characteristic of brachytherapy.

## References

1. Gulec S, Mesoloras G, and Stabin M. Dosimetric techniques in  $^{90}\text{Y}$ -microsphere therapy of liver cancer: the MIRD equations for dose calculations. *J Nucl Med.* 2006;47:1209-1211
2. Dezarn WA, Cessna JT, DeWerd LA, *et al.* Recommendations of the American Association of Physicists in Medicine on dosimetry, imaging, and quality assurance procedures for  $^{90}\text{Y}$  microsphere brachytherapy in the treatment of hepatic malignancies. *Med Phys.* 2011; 38(8):4824-4845
3. Potrebko PS, Shridhar R, Biagioli MC, Sensakovic WF, Andl G, Poleszczuk J, and Fox TH. SPECT/CT image-based dosimetry for Yttrium-90 radionuclide therapy: Application to treatment response. *J Appl Clin Med Phys.* 2018 Jul 1.
4. Siman W, Mikell JK, and Kappadath SC. Practical reconstruction protocol for quantitative  $^{90}\text{Y}$  bremsstrahlung SPECT/CT. *Med Phys.* 2016;43(9):5093-5103
5. Srinivas S, Natarajan N, Kuroiwa J, *et al.* Determination of radiation absorbed dose to primary liver tumors and normal liver tissue using post-radioembolization  $^{90}\text{Y}$  PET. *Front Oncol.* 2014;4(255)
6. Pasciak AS, Bourgeois AC, and Bradley YC. A comparison of techniques for  $^{90}\text{Y}$  PET/CT image-based dosimetry following radioembolization with resin microspheres. *Front Oncol.* 2014; 4(121)
7. Pasciak AS, Bourgeois AC, McKinney JM, Chang TT, Osborne DR, Acuff SN, and Bradley YC. Radioembolization and the dynamic role of  $^{90}\text{Y}$  PET/CT. *Front Oncol.* 2014; 4(38)
8. van Elmbt L, Walrand S, Lhommel R, Jamar F, and Pauwels S. Quantitative comparison between LYSO and BGO PET-tomographs in  $^{90}\text{Y}$  imaging. *EJNMMI.* 2010;37:S293-S293
9. Pacilio M, Amato E, Lanconelli N, *et al.* Differences in 3D dose distributions due to calculation method of voxel S-values and the influence of image blurring in SPECT. *Phys Med Biol.* 2015;60:1945-1964
10. Chiesa C, Mira M, Maccauro M, *et al.* Radioembolization of hepatocarcinoma with  $^{90}\text{Y}$  glass microspheres: development of an individualized treatment planning strategy based on dosimetry and radiobiology. *EJNMMI.* 2015;42(11):1718-1738
11. Pasciak AS, and Erwin WD. Effect of voxel size and computation method on Tc-99m MAA SPECT/CT-based dose estimation for Y-90 microsphere therapy. *IEEE Trans Med Imaging.* 2009;28(11):1754-8
12. Elschot M, Vermolen BJ, Lam MGEH, *et al.* Quantitative comparison of PET and bremsstrahlung SPECT for imaging the in vivo Yttrium-90 microsphere distribution after liver radioembolization. *PLoS One.* 2013;8(2):e55742

Radiation therapy is not appropriate for all cancers. For more information, please visit [www.varian.com/safety](http://www.varian.com/safety).

**varian**

[varian.com](http://varian.com)

USA, Corporate  
Headquarters and  
Manufacturer

Varian Medical Systems  
Palo Alto, CA  
Tel: 650.424.5700  
800.544.4636

Authorized Representative  
in the EU

Varian Medical Systems  
Nederland B.V.  
Houten, The Netherlands  
[customer.relations@varian.com](mailto:customer.relations@varian.com)

Headquarters Europe,  
Eastern Europe, Middle &  
Near East, India, Africa

Varian Medical Systems  
International AG  
Stienhausen, Switzerland  
Tel: 41.41.749.8844

Asia Pacific Headquarters

Varian Medical Systems  
Pacific, Inc  
Kowloon, Hong Kong  
Tel: 852.2724.2836

Australasian Headquarters

Varian Medical Systems  
Australasia Pty Ltd.  
Sydney, Australia  
Tel: 61.2.9485.0111

Latin American Headquarters

Varian Medical Systems  
Brasil Ltda.  
São Paulo, Brasil  
Tel: 55.11.3457.2655

Varian Medical Systems as a medical device manufacturer cannot and does not recommend specific treatment approaches. Specifications subject to change without notice. Not all features or products are available in all markets and are subject to change.

© 2019 Varian Medical Systems, Inc. All rights reserved. Varian and Varian Medical Systems are registered trademarks and RapidShare is a trademark of Varian Medical Systems, Inc. The names of other companies and products mentioned herein are used for identification purposes only and may be trademarks or registered trademarks of their respective owners.